Middle-East Journal of Scientific Research 15 (6): 834-839, 2013
ISSN 1990-9233

DOI: 10.5829/idosi.mejsr.2013.15.6.11326

Thermal Annealing Effect on the Structural and Magnetic Properties of Barium Hexaferrite Powders

A. Mahgoob and A.Y. Hudeish

Physics Department, Hodeidah University, Hodeidah, Yemen

Abstract: Samples examined in this experimental work were in the form of hexagonal barium ferrite with various temperatures annealing. Barium hexaferrite ($BaFe_{12}O_{19}$), is of great importance as permanent magnets, particularly for magnetic recording as well as in microwave devices. The variation of the temperatures annealing was found to affect coercivity, mean effective anisotropy field, magnetic viscosity and switching field distribution. Moreover the variation of interaction fields with various temperatures was found to be non linear and this can be attributed to the particle interactions in these systems. Single phase of well crystalline $BaFe_{12}O_{19}$ was first obtained at annealing temperature 1100°C. The SEM results showed that the grains were regular hexagonal platelets. In addition, maximum saturation magnetization was observed at annealing temperature 1200°C. However, it was found that the coercivety of the synthesized $BaFe_{12}O_{19}$ samples were lower than the theoretical values.

Key words: Thermal annealing · Barium hexaferrite · Magnetic properties · Crystalline size

INTRODUCTION

Hexagonal ferrites, $MFe_{12}O_{19}$, (where M=Ba, Sr and/or Pb) are a group of magnetic compounds, which all have high resistivity, magneto-crystalline anisotropy and saturation magnetization, low dielectric losses and are thermally stable well above their Curie temperature [1, 2]. The hexagonal M-type hard ferrites have attracted much attention as the most widely used permanent magnets, which account for about 90% of the annual production of the permanent magnets due to the good combination of high magnetic properties, chemical stability and low cost. Moreover, M-type hexaferrites have widely used in telecommunication, magnetic recording media, magneto-optics and microwave devices [1,3]. As a result of its specific magnetic properties, barium hexaferrite and its derivatives can be used for permanent magnets, magnetic recording media and microwave applications [4]. $BaFe_{12}O_{19}$ (BaM) and its derivatives are currently magnetic material with great scientific and technological interest, due to its relatively high curie temperature, high coercive force and high magnetic anisotropy field as well as an excellent chemical stability and corrosion resistivity [1]. Barium hexaferrite ($BaFe_{12}O_{19}$) has a complex hexagonal unit cell and belonging to the magnetoplumbite structures [5]. The magnetic properties of hexagonal barium ferrite, ($BaFe_{12}O_{19}$), have been intensively investigated as a material for permanent magnets, high-density recording media and microwave devices [6, 7]. When various combinations, such as Co-Ti or Co-Sn, are substituted for some iron in barium ferrite particles, the magnetic properties substantially changes which greatly affects the magnetic stability in the media, which results in a time-dependent magnetic behavior. This time-dependent behavior is well known as the magnetic relaxation [8]. The reported theoretical calculated coercive force, saturation magnetization and curie temperature values for pure and single domain barium hexaferrite was 6700 Oe, 72 emu g^{-1} and 450°C, respectively [9, 10]. It is difficult to obtain ultrafine and monodispersed particles by the conmmercial ceramic method (solid-state reaction) which involves the firing of stoichiometric mixture of barium carbonate and iron oxide at high temperatures [11, 12]. In this respect, several low-temperatures chemical methods were investigated for the formation of ultrafine $BaFe_{12}O_{19}$ particles. These methods comprised co-precipitation [4, 13, 14], hydrothermal [15-17], sol-gel [12, 18-20], microemulsion [10], oxalate precursor [21], glass crystallization [22], sonochemical [23] and mechano-chemical activation [24].

Corresponding Author: A. Mahgoob, Department of Physics, Hodeidah University, Hodeidah, Yemen.

The oxalate precursor technique was found to be more suitable for synthesis of barium ferrite with single phase powder. Generally, at relatively high temperatures,the instability is produced by thermal activation that overcomes energy barriers between the metastable states [25, 26].

$$M(t) = M_0(2e^{-t/\tau} - 1) \quad (1)$$

where M_o is the initial magnetization and τ is the characteristic time of relaxation which usually evaluated from Arrhenius Neel law [27]:

$$\tau = \tau_0 e^{\Delta E/KT} \ (\tau_0 = 10^{-9} s) \quad (2)$$

where ΔE is the energy barrier which depends on anisotropy field and applied field.

The time dependence of magnetization can be generally approximated with the logarithmic law [28]:

$$M(t) = M_0 - S\ln(t/t_0) \quad (3)$$

where t_0 is a constant; S is the viscosity of the material and is applied field dependent. According to Street and Woolley [29], H_f can be given by:

$$H_f = \frac{S}{x_{irr}} \quad (4)$$

where X_{irr} is the irreversible susceptibility. The idea of fluctuation field led to the concept of activation volume (V_{ac}) which is usually defined by [30]:

$$V_\alpha = \frac{kT}{M_S H_f} \quad (5)$$

where, k is Boltzmann's constant, T is the absolute temperature and M_s the saturation magnetization [28]. In this paper, we report the interaction effects and magnetic relaxation study on hexagonal barium ferrite of the oxalate precursor technique with various temperatures anneling. Effects of annealing temperature on the synthesis of ferrite powders were investigated. The annealing temperature was controlled from 900-1200°C, magnetic viscosity coefficient, fluctuation field and activation volume was examined. The influence of inter-particle interactions is also discussed.

Experimental Details: In this work, the oxalate precursor method was applied for the preparation of Barium hexaferrite ($BaFe_{12}O_{19}$). Chemically grade ferric chloride ($FeCl_3$-$6H_2O$), barium chloride ($BaC_{l2}.H_2O$) and oxalic acid as source of organic were used as starting materials. The mixtures of barium chloride and ferric chloride solution firstly prepared and then stirred for 15 min on a hot-plate magnetic stirrer, followed by addition of an aqueous solution, which was evaporated to 80°C with constant stirring until dry and then dried in a dryer at 100°C overnight. The dried powders obtained as barium ferrite precursors. Differential Thermal Analyzer (DTA) analysis of various un-annealed precursors was carried out. The rate of heating was kept at 10°C min^{-1} between room temperature and 1000°C. The measurements were carried out in a current of argon atmosphere. For the formation of the barium ferrite phase, the dry precursors were annealed at the rate of 10°C min^{-1} in static air atmosphere up to different temperatures (900 -1200°C) and maintained at the temperature for annealed. The crystalline phases presented in the different annealed samples were identified by XRD on a Brucker axis D8 diffractometer using Cu-Kα (λ=1.5406) radiation and secondary monochromator in the range 2Ø from 10-80°. The ferrites particles morphologies were observed by Scanning Electron Microscope (SEM, JSM-5400). The magnetic properties of the ferrites were measured at room temperature using an ultra sensitive vibrating sample magnetometer (VSM model MicroMag^{TM} 3900 of Princeton Measurement Corp.) with a noise base of 5×10^{-6}emu. From the obtained hysteresis loops, the saturation Magnetization (M_s), remanence Magnetization (M_r) and Coercivity (H_c) were determined. The time dependences of the magnetization of these particles were measured in the presence of a magnetic field applied in the opposite direction to the previously applied and removed saturating field (10 kOe).

RESULTS AND DISCUSSION

Figure 1 shows the measured hysteresis loops for samples which annealed at 900°C, 1000°C and 1100°C. It is display the effect of annealing temperature on the hystersis loop of $BaFe_{12}O_{19}$ powders obtained from oxalate precursors. Figure 1 clearly shows the effects of annealing temperature where the loop for higher of annealing temperature is steeper than that for the less annealing temperature one. This is likely due to the presence of single domain of $BaFe_{12}O_{19}$ particles.

Table 1: Coercivity, mean effective anisotropy field, switching field distribution, fluctuation field at H_c and Activation volume at H_c for all samples examined for different temperatures (900-1200°C).

Temp.(°C)	Coercivity (H_c) Oe	Mean effective anisotropy field (H_{keff}) Oe	Switching field distribution	Fluctuation field at H_c (H_f)Oe	Activation volume at H_c (V_{ac}) 10^{-18} cm^3
900	1246.4	1700	0.291	13.2	9.442
1000	1312.4	1330	0.338	13.2	9.47
1100	1340.6	1187	0.336	12.7	9.853
1200	1373.8	1231	0.331	12.8	9.802

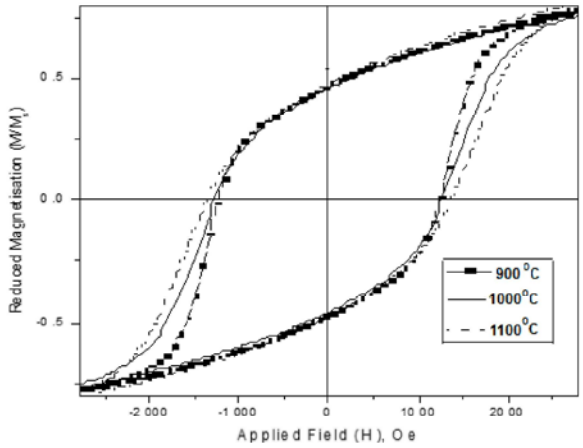

Fig. 1: The measured hysteresis loops for samples thermally treated at different temperatures (900-1100°C).

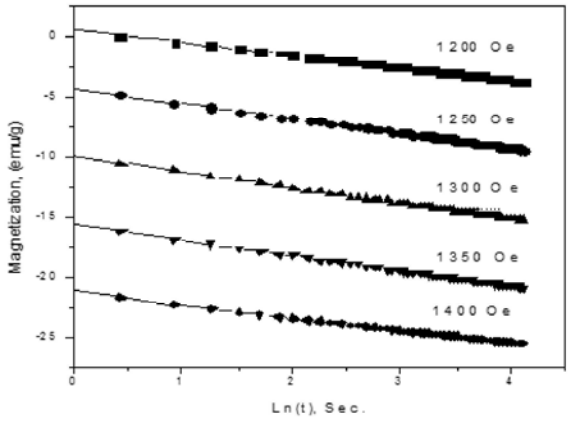

Fig. 2: The variation of magnetization with Ln(t) at various reverse applied fields for sample treated at (900°C).

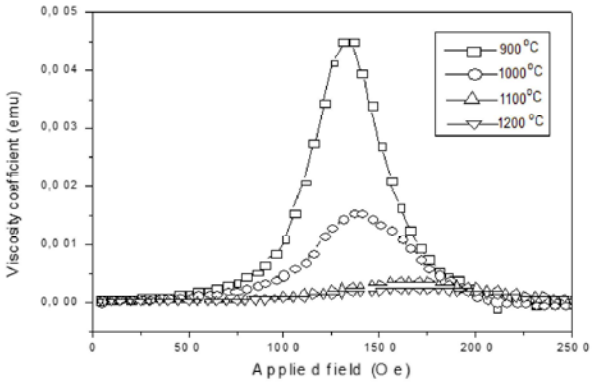

Fig. 3: The variation of magnetic viscosity coefficient with applied field for samples thermally treated at different temperatures (900-1200°C).

In line with SEM results, the change in magnetic properties can be attributed to the presence of well crystalline $BaFe_{12}O_{19}$ microstructures, as the annealing temperature of the powders was increasing gradually to reach optimum conditions. Also the measured hysteresis loops show that the remanence ratio is less than well known Stoner–Wohlfarth value (i.e. 0.5) [31,32]. This value suggests that the predominant dipolar interactions in these systems are negative which suppress the remanence ratio below 0.5. The coercivity (H_c) of all samples examined is listed in Table 1. With decreasing concentration, coercivity remarkably increases.

Fig.2 reports the typical evolution of the magnetization versus time with different negative applied fields near coercivity for 900°C sample. The logarithmic behavior is well observed in the full time range shown in Fig.2. It is seen that the decrease rate of the magnetization depends on the applied field. By fitting the linear behavior, the magnetic viscosity coefficient for all samples was obtained. The field dependences of magnetic viscosity for samples annealled at (900°C, 1000°C,1100°C and 1200°C) are shown in Fig. 3. All the curves are "bell Shaped" as defined by Mayergoyz *et al.* [33]. With the increase of annealing temperature, the maximum of magnetic viscosity increases which indicating the increase of magnetic thermal relaxation. This can be attributed to a decrease of the mean effective anisotropy field (H_{keff}) as shown in table (1). The actual switching field distributions (SFD), which were deducted from DCD curves as equal to $[H(m_d = 0.5) - H(m_d = -0.5)]/H_r$, are listed in table1, experimental details to obtain SFD were reported by Kodama [34]. In general here it is seen that,

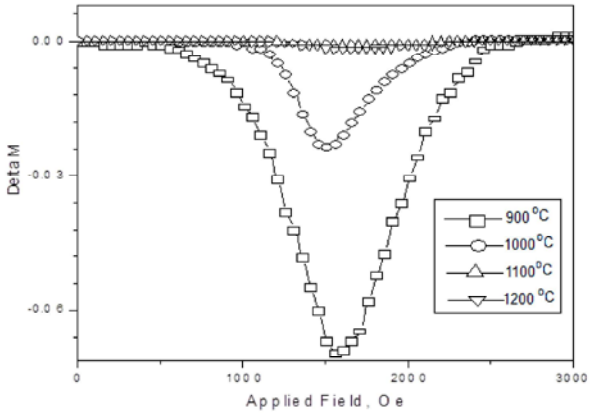

Fig. 4: The variation of $\Delta M$with applied field for some of the samples examined thermally treated at different temperatures (900-1200°C).

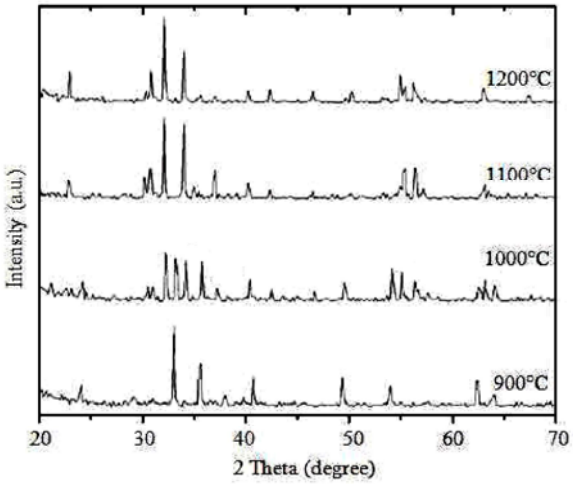

Fig. 5: XRD patterns of $BaFe_{12}O_{19}$ thermally treated at different annealing temperature.

widens the switching field distribution. Doping of barium ferrite powders with Co-Ti reduces the crystal anisotropy [35], so the reduction of crystal anisotropy after doping makes the shape anisotropy term more important, while the shape anisotropy is related to particle demagnetization factor, which is not a single value throughout the particle. This may produce a broadening of switching field distribution and increase magnetic relaxation. For a particle assembly, the particle interaction influences the magnetic relaxation process by changing the energy barrier distributions [36]. Fig. 4 showed the curves for the samples annealled at (900°C, 1000°C,1100°C and 1200°C). The negative value of demonstrates that the predominant interactions in ($BaFe_{12}O_{19}$) powder systems are negative (dipolar interactions). Also it is clear from these data that the change in with field for the ($BaFe_{12}O_{19}$) powder at (900°C) annealing temperature is steeper than the others samples at higher annealing temperatures. This behavior suggests that the interaction driven changes in the remanence states in the powder sample occurs different annealing temperature as a result of particle stacking. So Delta *M* is observed to be more negative with the reduction of the annealing temperatures. For further reduction in the annealing temperatures the profile becomes less negative due to the decrease in the predominant negative dipolar interactions. According to Pfeiffer [37], the influence of the interparticle interaction can be evaluated by a parameter of mean interaction field H_{int}, which could be estimated as $1/2(H_r^{/} - H_r)$. Where H_r and $H_r^{/}$ correspond to the remanent coercivity on the DCD and IRM curves, respectively, for the details pleas refer to [37]. Again the behaviour of the interaction field in these systems can be mainly attributed to the behaviour of predominate dipolar interactions. The fluctuation field at the coercivity for all samples examined which calculated according to Eqs. (4) are listed in Table 1. Activation volume at the coercivity was obtained by substituting the values of fluctuation fields in Eqs. (5) (Table 1). Principally, the thermal activation volume constitutes an estimate of the volume of material involved in a single activation process. If the particle reverses by coherent rotation, V_{ac} should be equal to the particles physical volume ($1.2\times10^{-17} cm^3$). For the above samples, we found that the calculated V_{ac} is about 60 % of the physical volume. This means that the reversal mechanism is rather incoherent in these powder systems [25].

Fig. 5 shows the XRD patterns of the calcined powder of $BaFe_{12}O_{19}$ obtained from barium-iron oxalate precursor solutions, with thermally treated at different temperatures (900-1200°C). On the start of the annealing process at (900°C), a complete absence of M-type barium ferrite phase. Instead, the hematite Fe_2O_3 phase appears as a major phase, which is consistent with DTA results. But at (1000°C) the concentration of the hematite phase decreases and barium ferrite phase was detected. Increasing the annealing temperature to 1100°C, enhanced the formation of barium hexaferrite phase and decreased the hematite Fe_2O_3 phase. At the calcinations temperature (1200°C), single phase of barium hexaferrite ($BaFe_{12}O_{19}$) evidently was formed XRD analysis was carried out in this study to investigate the effect of the powders thermally treated at different temperatures (900-1200°C). Fig. 6 shows the effect of various annealing temperature on the crystalline size of the obtained powders. It can be observed that increasing the annealing temperatures helps significantly agglomeration of the particles and

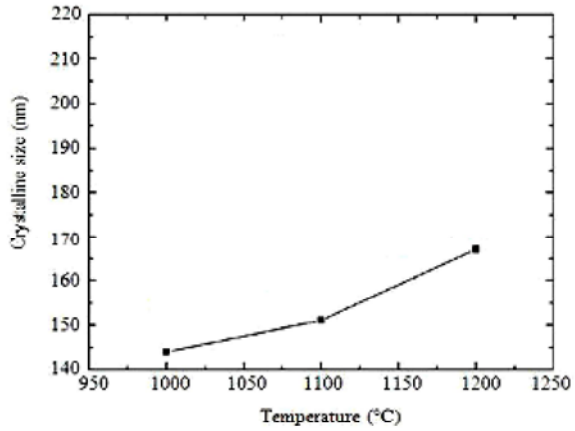

Fig. 6: Effect of annealing temperature on the crystalline size of the prepared barium hexaferrite.

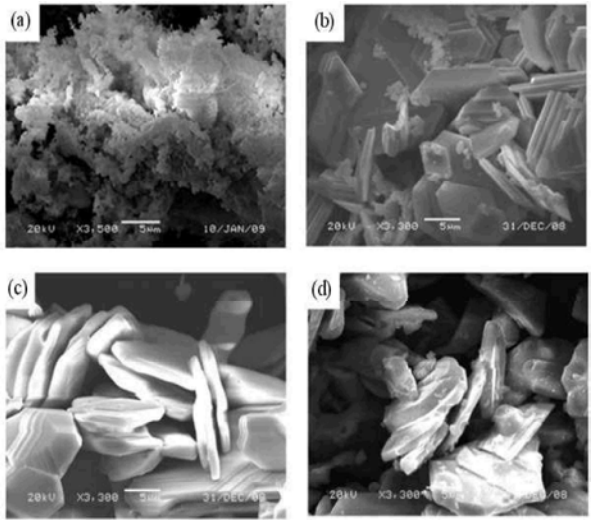

Fig. 7: SEM micrographs of $BaFe_{12}O_{19}$ powders obtained from oxalate precursors with annealing temperature. (a) 900°C; (b) 1000°C; (c) 1100°C; (d) 1200°C.

grains growth during calcination course, which leads to the increase of grain size and formation of single phase barium hexaferrite powders. Fig. 7 displays SEM micrographs of $BaFe_{12}O_{19}$ powders obtained from oxalate precursors with annealedtemperatures. In Fig. 7a, fine precipitated particles, with random grain orientation. This confirms the previous results of XRD and DTA, which showed no sign of $BaFe_{12}O_{19}$ growth at 900°C. However, as the annealing temperatures increased to 1000°C Fig. 7b, individual particles possess a plate-like hexagonal shape containing a fewer numbers of spherical small particles. At annealing temperature 1100°C (Fig. 7c), the ferrite powders showed uniform coarse structure with a well-clear hexagonal shape which is in line with XRD patterns in Fig. 5, for where pure single crystal peaks of barium ferrite was very evident. The grains were then started to distort again at 1200°C (Fig. 7d), which may lead to agglomeration of the particles at more higher annealing temperatures.

CONCLUSIONS

The magnetic relaxation at varius temperature annealing has been studied on Barium hexaferrite ($BaFe_{12}O_{19}$) powder at thermally treated at different annealing temperatures. Differential Thermal Analysis (DTA) plots of the synthesized mixture of barium-iron oxalates precursors showed the single phase of well crystalline $BaFe_{12}O_{19}$ was first obtained at annealing temperature 1100°C. By increasing the temperature up to 1200°C, grains have coalesced to form larger grains. The oxalate precursor route has proven to produce pure barium ferrite powders with good magnetic properties with increasing temperature, the maximum of magnetic viscosity increased. This is mainly caused by the decrease of mean effective anisotropy field. The interparticle interaction was found to be demagnetizing. The variation of interaction field with different temperatures found to be non linear, which is consistent with the delta M data. The calculated activation volume was 60% of the particles physical volume, indicating incoherent magnetic reversals in Barium hexaferrite ($BaFe_{12}O_{19}$) powders. Regarding the particles size, it can be seen that, the minimum particle size appeared at (1000°C) and the maximum size was found at (1200°C), which most likely explained by the formation of the single phase of barium hexaferrite $BaFe_{12}O_{19}$.

REFERENCES:

1. Kojimi, H. and E.P. Wohlfarth, 1982. Ferromagnetic Materials. North Holland, Amsterdam, pp: 305.
2. Smit, J. and H.P.J. Wijn, 1959. Ferrites: Physical Properties of Ferrimagnetic Oxides in Relation to their Technical Applications. NV Philips' Technical Library, Eindhoven, pp: 369.
3. Ogasawara, T. and M.A.S. Oliveira, 2000. Microstructure and hysteresis curves of the barium hexaferrite from co-precipitation by organic agent, J. Magn. Magn. Mater., 217: 147-154.
4. Hessien, M.M., 2008. Synthesis and characterization of lithium ferrite by oxalate precursor route. J. Mag. Magn. Mater., 320: 2800-2807.

5. Richerson, D.R., 1992. Modern Ceramic Engineering. 2nd Edn., Marcel Dekker. Inc., NY., ISBN: 0-8247-8634-3, pp: 294.
6. Magn, M.J. and Mate Magn, 1988. 74: 193.
7. Zeina, N., H. How, C. Vittoria and R. West, 1992. IEEE Trans. Magn, 28: 3219.
8. Chantrell, R.W. and J. Magn, 1991. Magn Mater, 9: 365.
9. Miller, J.S. and M. Drillon, 2002. Magnetism: Molecules to Materials III. Wiley-VCH Verlag GmbH, ISBN: 3527-30302-2, pp: 37.
10. Pillai, P., P. Kumar, M.S. Multani and D.O. Shah, 1993. Structure and magnetic properties of nanoparticles of barium ferrite synthesized using microemulsion processing. Colloids Surf. A: Physi-Cochem. Eng. Aspects, 80: 69-75.
11. Cabaoas, M.V. and J.M. Gonzalez-Calbet, 1993. Influence of the synthetic route on the $BaFe_{12}O_{19}$ properties. Solid State Ionics, 63-65: 207-212.
12. Bahgat, M., M. Radwan and M.M. Hessien, 2007. Reduction behavior of barium hexaferrite into metallic iron nanocrystallites, J. Magn. Magn. Mater, 310: 107-115.
13. Jacobo, S.E., L. Civale, C. Domingo-Pascual, R. Rodrigues-Clements and M.A. Blesa, 1997.
14. Matutes-Aquino, J., S. Dyaz-Castanon, M. Mirabal-Garcya and S.A. Palomares-Sanchez, 2000. Synthesis by coprecipitation and study of barium hexaferrite powders. Scripta Mater., 42: 295-299.
15. Wang, M.L., Z.W. Shih and C.H. Lin, 1993. Reaction mechanism producing barium hexaferrites from goethite and barium hydroxide by hydrothermal method. J. Cryst. Growth, 130: 153-161.
16. Liu, X., J. Wang, L.M. Gan and S.C. Ng, 1999. Improving the magnetic properties of hydrothermally synthesized barium ferrite. J. Magn. Magn. Mater., 195: 452-459.
17. Mishra, D., S. Anand, R.K. Panda and R.P. Das, 2004. Studies on characterization, microstructures and magnetic properties of nano-size barium hexa-ferrite prepared through a hydrothermal precipitation-calcination route. Mater. Chem. Phys., 86: 132-136.
18. Surig, C., K.A. Hempel and C. Sauer, 1996. Influence of stoichiometry on hexaferrite structure. J. Magn. Magn. Mater., 157-158: 268-269.
19. Zhong, W., W. Ding, N. Zhang, J. Hong, Q. Yan and Y. Du, 1997. Key step in synthesis of ultrafine BaFe12O19 by sol-gel technique. J. Magn. Magn. Mater., 168: 196-202.
20. Garcia, R.M., E.R. Ruiz, E.E. Rams and R.M. Sanchez, 2001. Effect of precursor milling on magnetic and structural properties of $BaFe_{12}O_{19}$ M-ferrite. J. Magn. Magn. Mater., 223: 133-137.
21. Sankaranarayanan, V.K. and D.C. Khan, 1996. Mechanism of the formation of nanoscale M-type barium hexaferrite in the citrate precursor method. J. Magn. Magn. Mater., 153: 337-346.
22. El-Hilo, M., H. Pfeiffer, K.O. Grady, W. Schuppel and E. Sinn *et al.*, 1994. Magnetic properties of barium hexaferrite powders. J. Magn. Magn. Mater., 129: 339-347.
23. Shafi, K.V.P.M. and A. Gedanken, 1999. Sonochemical approach to the preparation of barium hexaferrite nanoparticles. Nanostruct. Mater., 12: 29-34.
24. Abe, O. and M. Narita, 1997. Mechanochemically assisted preparation process of barium hexaferrite powders. Solid State Ionics, 103: 101-103.
25. Mohsen, Q., 2010, Factors Affecting the Synthesis and Formation of Single-Phase Barium Hexaferrite by a Technique of Oxalate Precursor, A. J. Appl. Sci., 7(7): 914-921.
26. Rashad, M.M. and Ibrahim, I.A., 2011. Improvement of the magnetic properties of barium hexaferrite nanopowders using modified co-precipitation method, J. Magn. Magn. Mater. 323: 2158–2164. Journal of Magnetism and Magnetic Materials, 323: 2158-2164.
27. Neel, L., 1955. Adv. Phys., 4: 191.
28. Ong, C.K., H.C. Fang, Z. Yang, Y. Li and J. Magn, 2000. Magn. Mater., 213: 413-417.
29. Street, R. and J.C. Woolley, 1949. Proc. Phys. Soc. London, Sect, A 62: 562.
30. Wohlfarth, E.P. and J. Phys, 1998. F 14: L155.
31. Stoner, E.C. and E.P. Wohlfarth, 1948. Phil. Trans. Roy. Soc., A 240: 599.
32. Thamm, S. and J. Hesse, 1998. J. Magn. Magn. Mater., 184: 245-255.
33. Mayergoyz, I.D., A. Adly, C. Korman, Huang Mingwei, C. Krafft and J. Appl, 1999. Phys., 85: 4358.
34. Kodama, N., H. Inoue, G. Spratt, Y. Uesaka and M. Katsumoto, J. Appl, 1999. Phys, 69: 4490.
35. Zheng, Y., X.Z. Hua, H.H. De, L. Jian, L.G. Sheng and J. Magn, 1992. Magn. Mater, 115: 77-86.
36. Garcia a del Muro, M., X. Battle, A. Labarta, J.M. Gonzalez and M.I. Montero, 1997. J. Appl. Phys., 81: 3812.
37. Pfeiffer, H., 1990, Phys. Stat. Sol., A 118: 295.